Viscosity in the escape-rate formalism

S. Viscardy and P. Gaspard
Center for Nonlinear Phenomena and Complex Systems, Université Libre de Bruxelles, Campus Plaine, Code Postal 231, B-1050 Brussels, Belgium

(Received 7 February 2003; published 23 October 2003)

We apply the escape-rate formalism to compute the shear viscosity in terms of the chaotic properties of the underlying microscopic dynamics. A first-passage problem is set up for the escape of the Helfand moment associated with viscosity out of an interval delimited by absorbing boundaries. At the microscopic level of description, the absorbing boundaries generate a fractal repeller. The fractal dimensions of this repeller are directly related to the shear viscosity and the Lyapunov exponent, which allows us to compute its values. We apply this method to the Bunimovich-Spohn minimal model of viscosity which is composed of two hard disks in elastic collision on a torus. These values are in excellent agreement with the values obtained by other methods such as the Green-Kubo and Einstein-Helfand formulas.

DOI: 10.1103/PhysRevE.68.041205 PACS number(s): 05.60.−k, 05.45.Ac, 05.45.Df, 05.45.Jn

I. INTRODUCTION

The link between the irreversible phenomena governed by macroscopic equations such as the Navier-Stokes equations and the microscopic reversible dynamics of the atoms and molecules is a fundamental problem. In this context, it has been shown that typical many-body systems of interacting particles present a chaotic dynamics [1–4]. This microscopic chaos develops a sensitivity to initial conditions over a time scale of the order of the intercollisional time of the atoms and molecules. This sensitivity to initial conditions is characterized by positive Lyapunov exponents which are the rates of exponential separation between some reference and perturbed trajectories of the system. The sensitivity to initial conditions results into a huge dynamical randomness characterized by a positive Kolmogorov-Sinai (KS) entropy per unit time given by the sum of positive Lyapunov exponents if the system is at equilibrium:

$$h_{\mathrm{KS}}=\sum_{\lambda_i>0}\lambda_i\,, \tag{1}$$

an identity known as Pesin's equality [5,6]. This dynamical chaos provides an efficient mechanism of randomization of the different observable quantities such as the microscopic currents associated with the transport properties.

For a Hamiltonian-type microscopic dynamics, a connection can be established between dynamical chaos and the transport properties, thanks to the escape-rate formalism [7–11]. In this formalism, the gap between the kinetic time scale of chaotic properties and the hydrodynamic time scale of transport properties is bridged by linking the transport coefficients to *differences* between chaotic properties. In this formalism, the following formula has been derived for viscosity [8]:

$$\eta=\lim_{\chi\to\infty}\left(\frac{\chi}{\pi}\right)^2\left(\sum_{\lambda_i>0}\lambda_i-h_{\mathrm{KS}}\right)_{\mathcal{F}_\chi}\,, \tag{2}$$

where the difference between the sum of positive Lyapunov exponents and the KS entropy is nonvanishing because the system is here under *nonequilibrium* conditions. These nonequilibrium conditions select the trajectories of the many-body system which do not escape out of a phase-space region specific to the transport property of interest. This phase-space region is defined by requiring that the Helfand moment associated with the transport property remains bounded in an interval of extension χ. In the limit $\chi\to\infty$, the nonequilibrium condition is progressively relaxed and the sum of positive Lyapunov exponents as well as the KS entropy approach their equilibrium value satisfying Pesin's equality (1). Under nonequilibrium conditions, Pesin's equality is not satisfied and the difference gives the rate of escape of trajectories out of the aforementioned phase-space region [5,12]. This region contains a fractal repeller $\mathcal{F}_\chi$ composed of trajectories which escape neither in future nor in past. The escape rate is characteristic of this fractal repeller and is related to the transport coefficient, leading to formula (2). The escape-rate formalism has already been applied to the transport property of diffusion [13] as well as to reaction-diffusion processes [14,15].

The purpose of the present paper is to apply the escape-rate formalism to viscosity. The system we use as a vehicle of our study is a minimal model of viscosity previously analyzed by Bunimovich and Spohn [16]. The minimal models of transport are of special interest because they are the simplest possible models already presenting a positive and finite transport coefficient. It is known that a minimal model should contain only one particle for diffusion, two particles for viscosity, and three particles for heat conduction [16]. For viscosity, we therefore consider here the model composed of two hard disks moving on a torus and undergoing elastic collisions. In a previous paper [17], we have described this model and some of its properties for a hexagonal geometry and a square geometry. Our aim here is to compute viscosity, thanks to the escape-rate formalism, and to show the equivalence with the results of the Green-Kubo and Einstein-Helfand formulas already obtained in the previous paper [17].

In the present paper, we compute the viscosity by using the chaotic and fractal properties of the repeller. We use a variant of Eq. (2) in which the difference between positive Lyapunov exponents and KS entropy is given in terms of the Lyapunov exponents and the partial fractal dimensions of the fractal repeller. Indeed, the fractality of the repeller is a corollary of its chaoticity so that its fractal dimensions are related to its KS entropy. Accordingly, the knowledge of the partial dimensions allow us to evaluate the KS entropy.

The paper is organized as follows. In Sec. II, we develop the escape-rate formalism for shear viscosity. In Sec. III, we present the fractal repeller of viscosity in the two-disk model, which we compare with the fractal repeller of diffusion in the Lorentz gas. In this way, we show that a specific fractal repeller is associated with each transport property. Finally, the chaotic and fractal properties are described in Sec. IV where we compute the viscosity coefficient from the positive Lyapunov exponent and the fractal dimension of the repeller. Conclusions are drawn in Sec. V.

II. VISCOSITY IN THE ESCAPE-RATE FORMALISM

A. Helfand moment for viscosity

In the previous paper [17], we have shown that the shear viscosity coefficient can be computed with the Einstein-Helfand formula [18]

$$\eta=\eta_{xy,xy}=\eta_{yx,yx}=\lim_{t\to\infty}\frac{1}{2t}\langle[\tilde{G}_{yx}(t)-\tilde{G}_{yx}(0)]^2\rangle, \quad (3)$$

where the Helfand moment is defined by

$$\tilde{G}_{yx}\equiv\sqrt{\frac{\beta}{V}}G_{yx}=\sqrt{\frac{\beta}{V}}\left[\sum_{a=1}^{N}x_a(t)p_{ay}(t)-\sum_{a=1}^{N}\sum_{s}\Delta x_a^{(s)}p_{ay}^{(s)}\theta(t-t_s)\right] \quad (4)$$

for a system of N particles of position $\mathbf{r}_a=(x_a,y_a,\dots)$ and momentum $\mathbf{p}_a=(p_{ax},p_{ay},\dots)$ moving in a domain delimited by periodic boundary conditions. As explained in the previous paper [17], the particles must satisfy the minimum image convention, which requires the presence of the extra terms in the Helfand moment (4) involving the jumps $\Delta x_a^{(s)}$ of the particles to fulfill the periodic boundary conditions. t_s are the times of the jumps. $p_{ay}^{(s)}=p_{ay}(t_s)$ is the momentum at the time t_s of the jump. In Eq. (3), the average $\langle\cdot\rangle$ is taken in the equilibrium microcanonical ensemble for which

$$\beta=\frac{N}{k_{\mathrm{B}}T(N-1)}. \quad (5)$$

B. First-passage problem for viscosity

The central object of the escape-rate formalism is the fractal repeller which is composed of the phase-space trajectories for which the Helfand moment fluctuates forever (in the future and the past) within some interval:

$$-\frac{\chi}{2}\leqslant\tilde{G}_{yx}\leqslant+\frac{\chi}{2}. \quad (6)$$

These trajectories are exceptional because the Helfand moment escapes out of this interval for almost all the trajectories. Therefore, the repeller has a vanishing probability measure in the phase space albeit it is typically composed of a nonenumerable set of trajectories. The repeller thus typically forms a fractal in the phase space [9,10].

We set up a first-passage problem of the Helfand moment by introducing absorbing boundaries at $\tilde{G}_{yx}=\pm\chi/2$. These absorbing boundaries in the space of variations of the Helfand moment correspond to equivalent absorbing boundaries in the phase space of the system. In the phase space, the absorbing boundaries delimit a domain which contains the fractal repeller. We consider a statistical ensemble of initial conditions taken inside this domain and we run their trajectories. When a trajectory reaches the absorbing boundaries it escapes out of the domain and is thus removed out of the statistical ensemble.

Under the forward time evolution, the remaining trajectories belong to the stable manifolds of the repeller. Under the backward time evolution, the remaining trajectories belong to the unstable manifolds of the repeller. Under both the forward and backward time evolutions, the remaining trajectories belong to the repeller itself which is the intersection of its stable and unstable manifolds [9]. For a typical chaotic dynamics, almost all trajectories escape out of the domain after some time so that the repeller as well as its stable or unstable manifolds are fractal objects.

These fractals can be generated by allowing the escape of trajectories over a long but finite time interval. Over a finite time, there remains a sizable set of trajectories, which progressively reduces to the fractal as the time interval becomes longer and longer. The number of trajectories in the set (or statistical ensemble) decays with time. Typically, the decay is exponential and characterized by the so-called escape rate γ.

The escape rate γ can be evaluated by solving the first-passage problem of the Helfand moment by introducing absorbing boundaries at $\tilde{G}_{yx}=\pm\chi/2$. Indeed, the Einstein-Helfand equation (3) shows that the Helfand moment performs a diffusivelike random walk. Accordingly, the Helfand moment can be considered as a random variable $g=\tilde{G}_{yx}$ for which the probability density $p(g)$ obeys a diffusion-type equation [8]:

$$\frac{\partial p}{\partial t}=\eta\frac{\partial^2 p}{\partial g^2}, \quad (7)$$

where the role of the diffusion coefficient is played by the shear viscosity (3) itself. At the absorbing boundaries, the probability density must satisfy the absorbing boundary conditions:

$$p\left(-\frac{\chi}{2}\right)=p\left(+\frac{\chi}{2}\right)=0. \quad (8)$$

The solution of the diffusion-type equation (7) with the boundary conditions (8) is given by

$$p(g,t)=\sum_{n=1}^{\infty} c_n \exp(-\gamma_n t)\sin\left[\frac{\pi n}{\chi}\left(g+\frac{\chi}{2}\right)\right], \tag{9}$$

with

$$\gamma_n=\eta\left(\frac{\pi n}{\chi}\right)^2, \tag{10}$$

and where the coefficient c_n depends on the initial probability density. The number $\mathcal{N}(t)$ of trajectories remaining between the absorbing boundaries at the current time t is related to the probability density by

$$\mathcal{N}(t)=\mathcal{N}_0\int_{-\chi/2}^{+\chi/2} p(g,t)dg\sim\mathcal{N}_0\exp(-\gamma_1 t). \tag{11}$$

After a long time, the escape is dominated by the smallest decay rate γ_1, which can therefore be identified with the escape rate γ. In this way, we obtain the *escape rate* as a function of χ:

$$\gamma=\gamma_1=\eta\left(\frac{\pi}{\chi}\right)^2. \tag{12}$$

This result is obtained by using the diffusion-type equation (7) which is expected to hold over spatial distances larger than the mean free path of the particles. Therefore, the parameter χ must be sufficiently large so that the Helfand moment is in a diffusion regime and Eq. (7) holds.

The shear viscosity coefficient can thus be obtained from the escape rate which depends on the parameter χ of separation between the absorbing boundaries as

$$\eta=\lim_{\chi\to\infty}\left(\frac{\chi}{\pi}\right)^2\gamma(\chi). \tag{13}$$

In the following we call Eq. (13) the escape-transport formula.

C. The chaos-transport formula

At the microscopic level of description, the escape rate is controlled by the fractal repeller $\mathcal{F}_\chi$ which is composed of all the trajectories which satisfy condition (6) under forward and backward time evolutions. The repeller is the support of a natural invariant probability measure. This invariant measure is natural because it is generated by the dynamics and can be approximated by a statistics based on the trajectories remaining within the absorbing boundaries after a long but finite time. The dynamics on the fractal repeller is characterized by positive Lyapunov exponents and a KS entropy, both evaluated with respect to the natural invariant measure of the repeller. If the dynamics is unstable some Lyapunov exponents are positive. If the dynamics is chaotic the KS entropy is positive. On a repeller, the sum of positive Lyapunov exponents differs from the KS entropy and the difference gives the escape rate $\gamma(\chi)$ of the repeller $\mathcal{F}_\chi$ [5,12]:

$$\gamma(\chi)=\left(\sum_{\lambda_i>0}\lambda_i-h_{\rm KS}\right)_{\mathcal{F}_\chi}. \tag{14}$$

If we combine this result from dynamical systems theory with Eq. (13), we obtain the chaos-transport formula (2) for viscosity as originally derived by Dorfman and Gaspard [8].

An equivalent formula can be obtained which involves the partial fractal dimensions of the repeller instead of the KS entropy. Indeed, the fractal character of the repeller is a direct consequence of the escape of trajectories so that the KS entropy is no longer equal to the sum of Lyapunov exponents but to

$$h_{\rm KS}=\sum_{\lambda_i>0} d_i\lambda_i, \tag{15}$$

where the coefficients are the partial information dimensions of the repeller associated with each unstable direction of corresponding Lyapunov exponent λ_i [5]. These partial dimensions satisfy

$$0\leqslant d_i\leqslant 1, \tag{16}$$

so that the KS entropy is in general smaller than the sum of positive Lyapunov exponents. Accordingly, the escape rate can be expressed as

$$\gamma(\chi)=\left(\sum_{\lambda_i>0} c_i\lambda_i\right)_{\mathcal{F}_\chi} \tag{17}$$

in terms of the partial codimensions defined as

$$c_i\equiv 1-d_i. \tag{18}$$

Combining with Eq. (13), the shear viscosity is given by

$$\eta=\lim_{\chi\to\infty}\left(\frac{\chi}{\pi}\right)^2\left(\sum_{\lambda_i>0} c_i\lambda_i\right)_{\mathcal{F}_\chi}. \tag{19}$$

In the limit $\chi\to\infty$, the Lyapunov exponents reach their equilibrium values $\lambda_{i,\rm eq}$, while the codimensions vanish typically as $c_i\sim\chi^{-2}$ if transport is normal. If we introduce the quantities

$$a_i\equiv\lim_{\chi\to\infty}\left(\frac{\chi}{\pi}\right)^2 c_i\Big|_{\mathcal{F}_\chi}, \tag{20}$$

Eq. (19) provides a decomposition of the viscosity coefficient on the spectrum of Lyapunov exponents such as

$$\eta=\sum_{\lambda_{i,\rm eq}>0} a_i\lambda_{i,\rm eq}. \tag{21}$$

Typically, the escape is most important in the most unstable direction corresponding to the maximum Lyapunov exponent λ_1. Therefore, the repeller is more depleted in the most unstable direction and the corresponding partial dimension d_1 is lower than the further ones. This reasoning suggests that a typical behavior is

$$\left(\sum_{\lambda_i>0} c_i\lambda_i\right)_{\mathcal{F}_\chi} \simeq (c_1\lambda_1)_{\mathcal{F}_\chi}, \tag{22}$$

for $\chi\to\infty$ if the maximum Lyapunov exponent λ_1 is well defined.

This is precisely the case in two-degree-of-freedom systems such as the two-disk model where the chaos-transport formula reduces to

$$\eta = \lim_{\chi\to\infty}\left(\frac{\chi}{\pi}\right)^2 (c_I\lambda)_{\mathcal{F}_\chi}, \tag{23}$$

where λ is the unique positive mean Lyapunov exponent and c_I the corresponding codimension which should be understood as the partial information codimension of the unstable manifolds of the fractal repeller given in terms of the partial information dimension by Young's formula [19]

$$c_I = 1 - d_I = 1 - \frac{h_{KS}}{\lambda}. \tag{24}$$

It is known that the partial information dimension of the repeller is well approximated by the partial Hausdorff dimension if the escape rate is small enough and if Ruelle's topological pressure does not present a discontinuity. This last condition is fulfilled if the system does not undergo a dynamical phase transition, which is the case in the finite-horizon regimes of Sinai's billiard which controls the dynamics of both the Lorentz gas and the two-disk model [13]. Under these conditions, we can replace the partial information codimension by the partial Hausdorff codimension in the chaos-transport formula and obtain the viscosity as

$$\eta = \lim_{\chi\to\infty}\left(\frac{\chi}{\pi}\right)^2 (c_H\lambda)_{\mathcal{F}_\chi}. \tag{25}$$

In the limit $\chi\to\infty$, the Lyapunov exponent converges to its equilibrium value so that we can also write

$$\eta = \lambda_{eq}\lim_{\chi\to\infty}\left(\frac{\chi}{\pi}\right)^2 c_H(\chi), \tag{26}$$

under similar conditions as Eq. (25).

III. FRACTAL REPELLER

In this section, our purpose is to display the fractal repeller associated with viscosity in the two-disk model and to compare it with the fractal repeller of diffusion in the Lorentz gas in order to show that they are different and therefore specific to each transport property.

A. Shear viscosity in the two-disk model

The two-disk model has been studied by Bunimovich and Spohn who proved, thanks to a central limit theorem, that viscosity is positive and finite in this minimal model [16]. In the previous paper [17], we have considered the two-disk model in the hexagonal geometry which we shall use in the following. We showed in Ref. [17] that the dynamics reduces to a Sinai billiard in the center-of-mass frame and that the Helfand moment (4) with $N=2$ is then given by

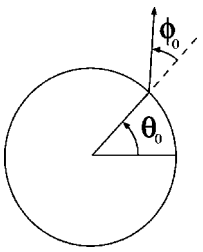

FIG. 1. Initial conditions of the particles in the Sinai billiard.

$$\tilde{G}_{yx}(t) = \sqrt{\frac{\beta}{V}}\left[x(t)p_y(t) - \sum_s \Delta x^{(s)} p_y^{(s)}\theta(t-t_s)\right], \tag{27}$$

where (x,y) are the coordinates of the relative position of both disks and (p_x,p_y) the canonically conjugated relative momentum. The jumps happen when the trajectory of Sinai's billiard crosses the hexagonal boundary. If the trajectory crosses the side of label ω the trajectory is reinjected at the opposite side so that the jump in position is given by the lattice vector $\Delta\mathbf{r}^{(s)} = -\mathbf{c}_\omega^{(s)}$ corresponding to the side ω.

A fractal repeller is defined by considering all the trajectories such that their Helfand moment satisfies the conditions

$$-\frac{\chi}{2} \leqslant \tilde{G}_{yx} \leqslant +\frac{\chi}{2}, \tag{28}$$

where the parameter χ should be large enough. The stable manifolds of the fractal repeller can be visualized by plotting the initial conditions of trajectories satisfying conditions (28) over a long time interval extending forward in time. These initial conditions are taken on the disk of Sinai's billiard. The initial conditions are specified by the angle θ of the initial position and the angle ϕ that the initial velocity makes with a vector which is normal to the disk at the initial position (see Fig. 1). The initial conditions are plotted in the Birkhoff coordinates $(\theta,\sin\phi)$.

Figure 2 depicts the fractal composed of the stable manifolds of the repeller for viscosity in the two-disk model. We provide evidence that the set is fractal by zooming successively on it in Figs. 3 and 4, where the self-similarity of the repeller clearly appears.

Let us take a section across the repeller in Fig. 2 at $\theta_0 = \pi/4$. Taking the escape time of the corresponding trajectory, we have obtained the escape-time function depicted in Fig. 5. The time for the trajectory to escape out of the phase-space region corresponding to interval (28) is infinite if the trajectory belongs to the stable manifold of a trajectory of the repeller. Indeed, this trajectory is then asymptotic to a trajec-

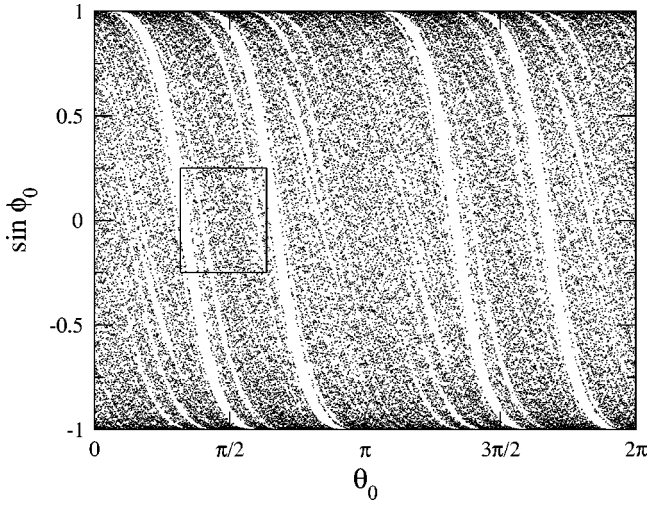

FIG. 2. Fractal repeller associated with viscosity in the hexagonal geometry with absorbing boundaries at $\chi = 2.70$. The density is $n = (2/V) = 0.45$.

tory which does not escape. Accordingly, the escape-time function has vertical asymptotes on the stable manifolds of the repeller. Since the repeller is fractal the vertical asymptotes are not enumerable, which explains the behavior in Fig. 5.

B. Diffusion in the Lorentz gas

Diffusion of a tracer particle in the hard-disk periodic Lorentz gas has been studied with the escape-rate formalism in Ref. [13]. In this Lorentz gas, the tracer particle undergoes elastic collisions on hard disks forming a triangular lattice. In a unit cell of the lattice, the dynamics also reduces to Sinai's billiard. The energy of the tracer particle is conserved as well as the phase-space volumes. Sinai and Bunimovich have proved that the dynamics is ergodic and mixing and that the diffusion coefficient is positive and finite in the finite-horizon regime [20]. For diffusion, the associated Helfand moment is simply given by one of the coordinates (x,y) of position of the tracer particle [8]. An escape process is associated with

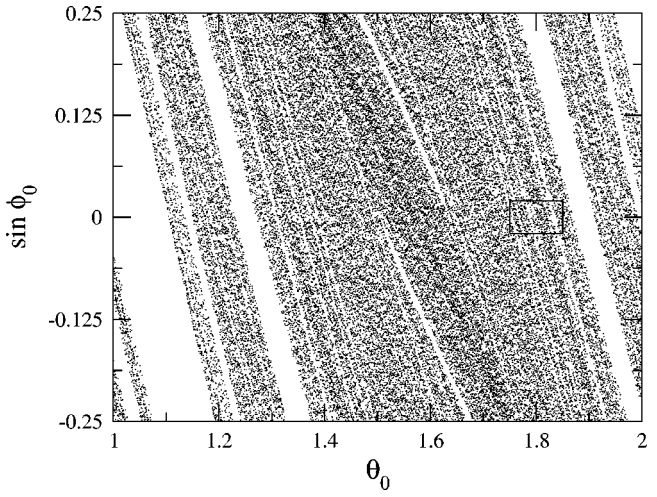

FIG. 3. Enlarging of the domain into the rectangle in Fig. 2.

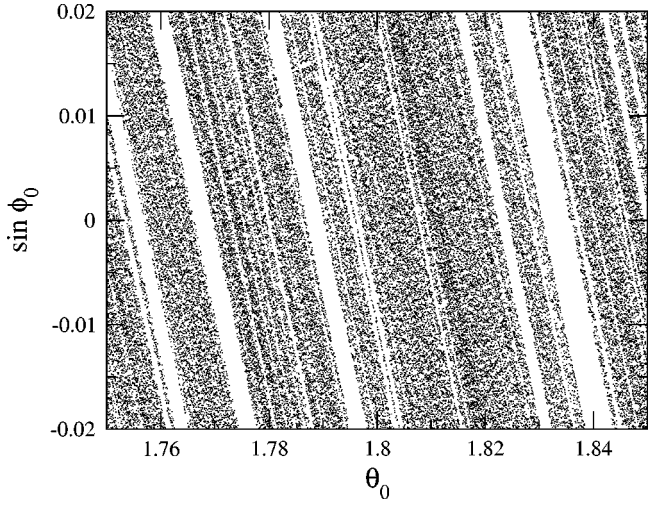

FIG. 4. Enlarging of the domain into the rectangle in Fig. 3.

diffusion by setting up a problem of first passage of the tracer particle at some absorbing boundaries. If we consider the x coordinates, the tracer particle does not escape as long as the following condition is satisfied:

$$-\frac{R}{2} \leqslant x \leqslant +\frac{R}{2}. \tag{29}$$

The absorbing boundary conditions are therefore defined at $x = \pm R/2$. With these absorbing boundaries, the system is called an *open Lorentz gas* [13].

The trajectories trapped within interval (29) form a fractal repeller as shown in Ref. [13]. In order to compare with the fractal repeller of viscosity, we can plot the fractal repeller of diffusion in a similar way as here above for viscosity (Fig. 6).

Here again, we plot all the initial conditions of trajectories remaining within interval (29) over a long forward time interval. These initial conditions are plotted in the same

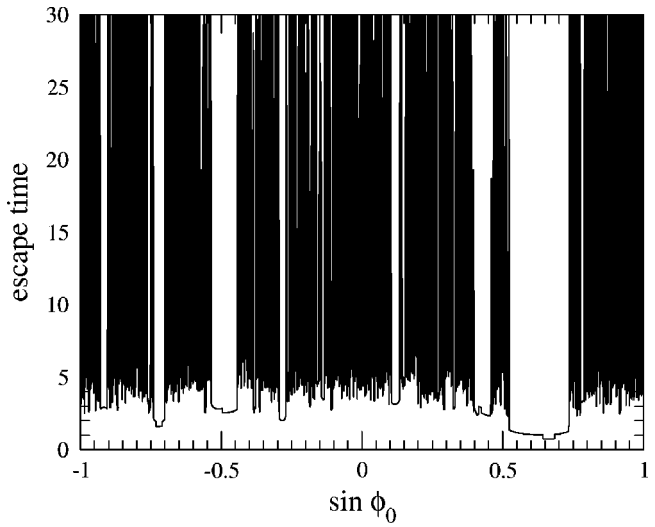

FIG. 5. Escape-time function vs sin ϕ_0 ($\theta_0 = \pi/4$). This function corresponds to a section in Fig. 2 along a vertical line at $\theta_0 = \pi/4$.

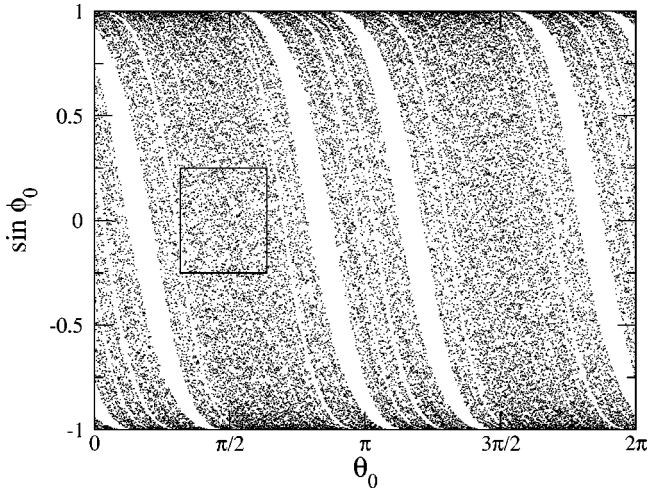

FIG. 6. Fractal repeller associated with diffusion in the hexagonal geometry with absorbing boundaries at $R=4$. The density of hard disks is $n=0.45$.

Birkhoff coordinates $(\theta,\sin\phi)$ of a disk around the coordinate $x\simeq 0$ in the Lorentz gas. The set of the selected initial conditions approximates the stable manifolds of the fractal repeller. We zoom successively on this fractal in Figs. 7 and 8, which provides evidence of its self-similarity. As a consequence, the repeller is also fractal. The fractal dimension of the repeller is related to the diffusion coefficient of the Lorentz gas and its Lyapunov exponent, as shown in Refs. [7,13].

C. Comparison between diffusion and viscosity

We observe that the two fractal repellers associated, respectively, with diffusion (see Fig. 6) and viscosity (see Fig. 2) are different. Indeed, although the global structure is similar, the trajectories belonging to the different repellers are not the same.

To convince us of this difference, we take some examples of trajectories. In Fig. 9, we have a periodic trajectory bouncing between two disks in the billiard. This trajectory belongs

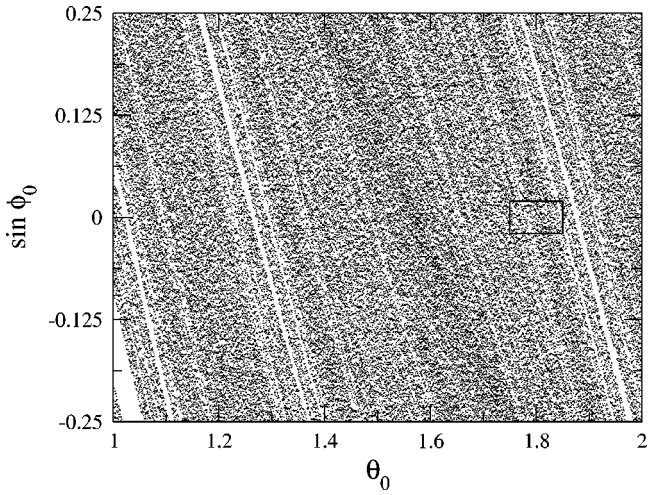

FIG. 7. Enlarging of the domain into the rectangle in Fig. 6.

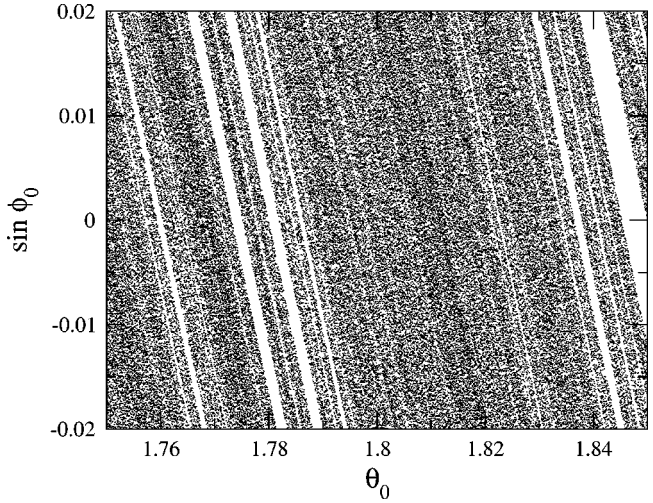

FIG. 8. Enlarging of the domain into the rectangle in Fig. 7.

to the repeller associated with diffusion since the position x is bounded and satisfied [Eq. (29)]. However, the viscosity Helfand moment of this trajectory does not satisfy condition (28) so that it does not belong to the repeller of shear viscosity. With Eq. (27), we see that, in one direction, both $\Delta x^{(s)}$ and $p_y^{(s)}$ are positive. Therefore, the contribution at this passage is positive for the Helfand moment. In the other direction, both $\Delta x^{(s)}$ and $p_y^{(s)}$ are negative but the product $\Delta x^{(s)}p_y^{(s)}$ is also positive. Accordingly, the Helfand moment increases forever on this trajectory which, therefore, does not belong to the repeller associated with shear viscosity.

On the other hand, we can observe the opposite case. Figure 10 depicts an example of trajectory escaping from interval (29) although its Helfand moment of viscosity remains between the absorbing boundary conditions (28).

The repellers associated with different transport properties are therefore different.

D. Escape rate and viscosity

In this section, we show that the shear viscosity can be obtained from the escape rate of the repeller by using the escape-transport formula (13). We consider a sequence of repellers with larger and larger values of the parameter χ. The escape rate $\gamma(\chi)$ is numerically evaluated for each re-

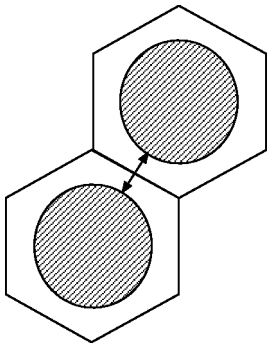

FIG. 9. Periodic trajectory belonging to the fractal repeller associated with diffusion but not to the one associated with viscosity.

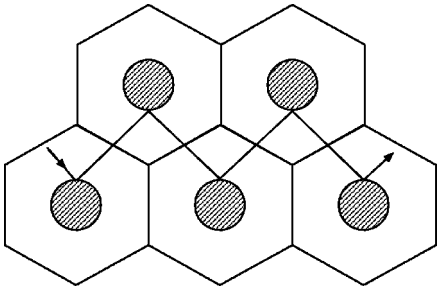

FIG. 10. Typical trajectory which moves through the whole system but which has a Helfand moment that remains close to zero. This trajectory belongs to the repeller of viscosity but not to the one of diffusion.

peller by computing the decay of the number $\mathcal{N}(t)$ of trajectories still within interval (28) at current time and by extracting the escape rate from the exponential decay. The escape rate is observed to behave as $\gamma(\chi)\sim\chi^{-2}$ and the shear viscosity coefficient is then obtained with Eq. (13).

Figures 11 and 12 depict the viscosity directly computed from the escape rate and compared with the values obtained by the Einstein-Helfand formula in Ref. [17] in the hexagonal and square geometries, respectively. As in the previous paper [17], we consider reduced viscosities defined by

$$\eta^*_{ij,kl}\equiv\frac{\eta_{ij,kl}}{2\sqrt{mk_BT}}. \tag{30}$$

We observe in Figs. 11 and 12 the excellent agreement between both methods.

IV. VISCOSITY FROM THE CHAOTIC AND FRACTAL PROPERTIES OF THE REPELLER

In this section, we compute the shear viscosity coefficient in terms of the chaotic and fractal properties of the repeller

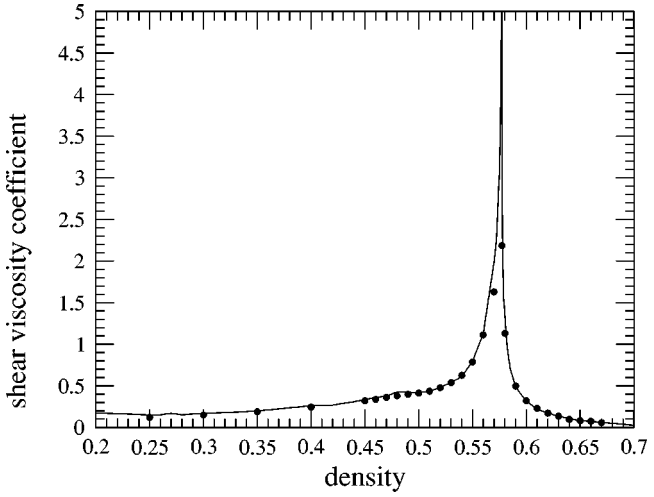

FIG. 11. Comparison between two methods of calculating the shear viscosity coefficient $\eta^*=\eta^*_{xy,xy}$ in the hexagonal geometry: the Einstein-Helfand formula (continuous line) and the escape-transport formula (13) with $\chi=60\sqrt{n}$ (dots).

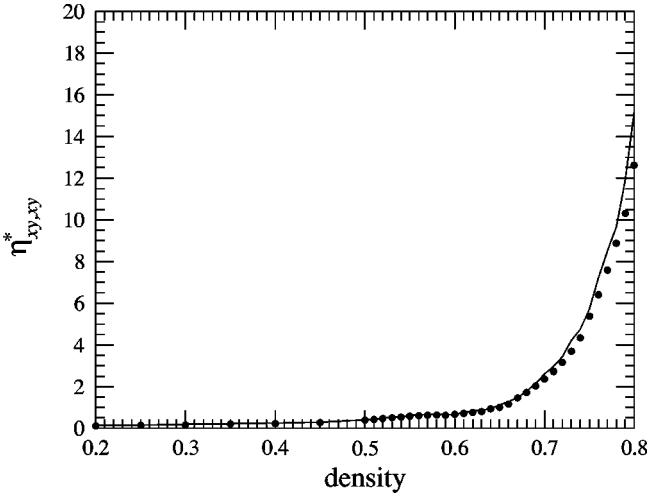

FIG. 12. Comparison between two methods of calculating the shear viscosity coefficient $\eta^*_{xy,xy}$ in the square geometry: the Einstein-Helfand formula (continuous line) and the escape-transport formula (13) with $\chi=45\sqrt{n}$ for density $n<0.66$, $\chi=100\sqrt{n}$ for $0.67<n<0.75$, and $\chi=150\sqrt{n}$ for $0.76<n$ (dots).

by using the chaos-transport formula (25) which related the viscosity to the Lyapunov exponent and the Hausdorff codimension of the repeller of viscosity.

A. Lyapunov exponent

In Sinai's billiard which controls the reduced dynamics of the two-disk model, the elastic collisions between the disks are defocusing. This induces a dynamical instability of the trajectories which is characterized by the Lyapunov exponents. These exponents are the rates of exponential separations between a reference orbit and infinitesimally close orbits. Since the dynamics of Sinai's billiard is symplectic and volume preserving in the four-dimensional phase space, the Lyapunov exponent spectrum is $(+\lambda,0,0,-\lambda)$ so that their sum is vanishing. One of the Lyapunov exponents vanishes because of the absence of exponential separation in the direction of the flow. Another one corresponding to the direction perpendicular to the energy shell equals zero because of energy conservation.

There exists a method to calculate the positive Lyapunov exponent by considering the motion of a front of particles accompanying the reference particle and issued from the same initial position but with different initial velocities [21]. Because the dynamics is defocusing, this front is expanding. Locally on the reference orbit Γ_t the front (called the unstable horocycle) is characterized by a curvature $\kappa_u(\Gamma_t)$ or, equivalently, by its radius of curvature $1/\kappa_u(\Gamma_t)$. Thanks to this method explained in detail in Refs. [10,13], we have computed the positive Lyapunov exponent as a function of the density of the system (in the hexagonal and square geometries). The equilibrium values of the Lyapunov exponent are obtained by running a trajectory in Sinai's billiard without absorbing boundaries and by averaging over a long time interval. The resulting numerical values are depicted in Figs. 13 and 14.

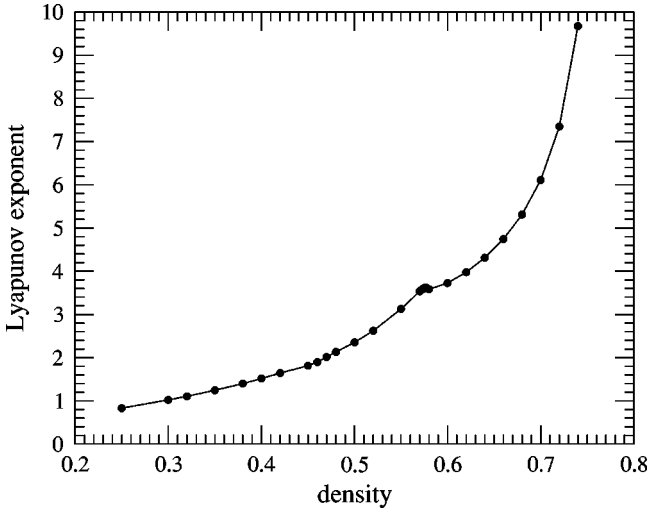

FIG. 13. Equilibrium Lyapunov exponent vs density in the hexagonal geometry.

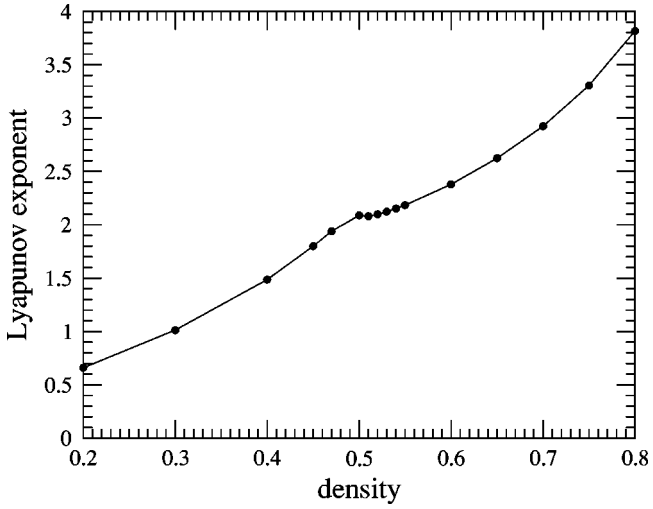

FIG. 14. Equilibrium Lyapunov exponent vs density in the square geometry.

In the chaos-transport formula (25), the Lyapunov exponent has to be evaluated for the trajectories belonging to the fractal repeller. The statistical average is here carried out for the natural invariant probability measure concentrated on the fractal repeller. This invariant measure defines a nonequilibrium state for the motion. As aforementioned, the natural invariant measure is generated by the dynamics itself. Accordingly, the Lyapunov exponent is numerically computed by averaging over a statistical ensemble of trajectories which has not yet escaped after a long but finite time. This ensemble can be as large as wished by increasing the number of initial conditions. In this way, we can calculate the nonequilibrium values of the Lyapunov exponent.

In Table I, we present a comparison between the equilibrium Lyapunov exponent λ_{eq} without absorbing boundary conditions (as depicted in Figs. 13 and 14) and the nonequilibrium Lyapunov exponent $\lambda_{neq}(\chi)$ evaluated over a nonequilibrium measure which has the fractal repeller as support. The difference between these exponents is small and of the order of the escape rate, in agreement with the results of Ref. [22] for the disordered Lorentz gas.

B. Hausdorff dimension and viscosity

In order to determine the viscosity by the chaos-transport formula (25), we need to determine the partial Hausdorff codimension c_H of the fractal repeller. The corresponding dimension $d_H=1-c_H$ is the Hausdorff dimension of the vertical asymptotes of the escape-time function depicted in Fig. 5. Its values range in the interval $0\leqslant d_H\leqslant 1$.

The Hausdorff codimension can be obtained using the following numerical algorithm developed by McDonald *et al.* [23]. We consider an ensemble of pairs of trajectories starting from initial conditions ϕ_0 differing in a value ϵ. The time taken by the trajectories to escape out of the system is given by the escape-time function in Fig. 5. The pair is said to be *uncertain* if the trajectories and their Helfand moment present at least one of the following conditions: (i) both trajectories follow paths that differ by the successive passages through the cell boundaries, that is, if we associate to each trajectory a symbolic sequence $(\omega_1,\omega_2,\ldots)$ which gives the labels of the cell boundaries across which the successive passages occur, and both sequences are different; (ii) one of both trajectories has its Helfand moment which reaches the fixed absorbing boundaries (28) when the Helfand moment of the other one still remains within these limits. If the pair does not present one of these conditions it is called *certain*. The fraction $f(\epsilon)$ of uncertain pairs in the initial ensemble is known to behave as the power

$$f(\epsilon)\sim\epsilon^{c_H}, \tag{31}$$

giving the Hausdorff codimension as its exponent. Deriva-

TABLE I. Values of the characteristic quantities of chaos for different densities n in the hexagonal system: λ_{eq} is the equilibrium Lyapunov exponent for the closed system. The following quantities characterize the fractal repeller for viscosity with $\chi=60\sqrt{n}$: λ_{neq} is the nonequilibrium Lyapunov exponent of the repeller, h_{KS} its KS entropy, γ its escape rate, c_I its partial information codimension, and c_H its partial Hausdorff codimension.

n	λ_{eq}	λ_{neq}	γ	$h_{KS}=\lambda_{neq}-\gamma$	$c_I=\gamma/\lambda_{neq}$	c_H
0.40	1.5156	1.5163	0.0017	1.5146	0.0011	0.0011
0.50	2.3519	2.3539	0.0023	2.3516	0.00098	0.00092
0.60	3.7258	3.7249	0.0015	3.7234	0.00040	

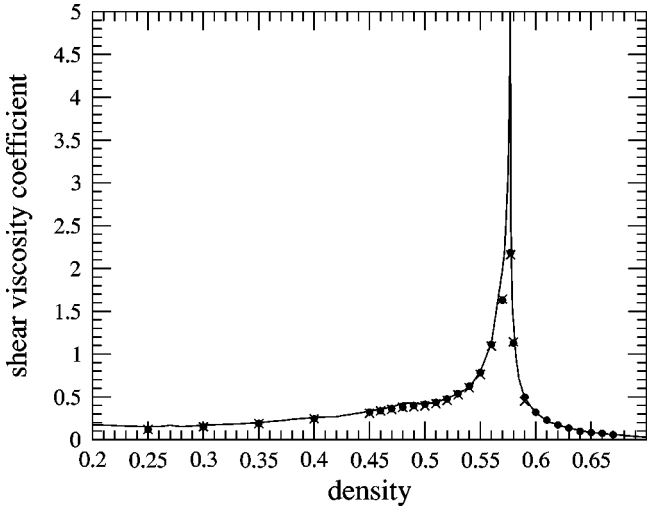

FIG. 15. Comparison between the three methods calculating the shear viscosity coefficient η^* in the hexagonal geometry: the Einstein-Helfand formula (3) (continuous line), the escape-transport formula (13) (dots), and the chaos-transport formula (25) (crosses) with $\chi=60\sqrt{n}$.

tions of this result can be found elsewhere [6,15,23]. This method has been already used in Refs. [13–15].

We have here applied the Maryland algorithm to obtain the Hausdorff codimension of the fractal repeller of viscosity. Table I compares the partial Hausdorff codimension with the partial information dimension in particular cases. We observe that both codimensions take very close values as expected.

By varying the parameter χ, we have obtained the shear viscosity, thanks to the chaos-transport formula (25). These values are plotted in Figs. 15 and 16 for the hexagonal and square geometries, respectively. We consider the shear viscosity coefficient η^* in the hexagonal geometry and the element $\eta_{xy,xy*}$ of the viscosity tensor in the square geometry. The values obtained with the chaos-transport formula (25) are compared with the values obtained by the escape-transport formula (13) and those by the Einstein-Helfand formula (3) obtained in the previous paper [17]. The agreement between the three formulas is excellent, which confirms the theoretical results.

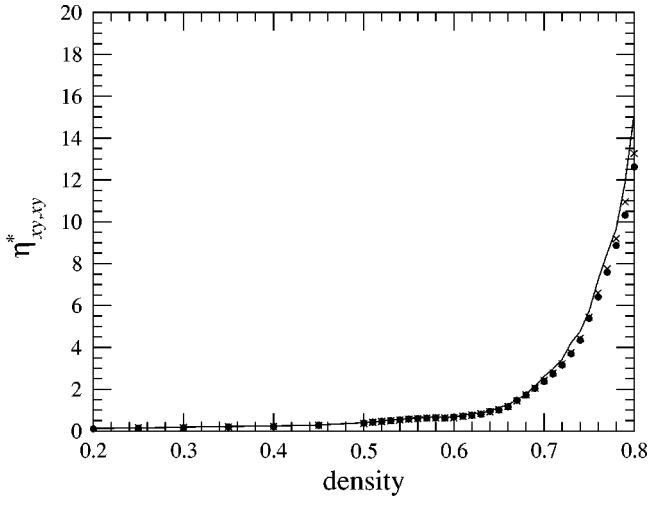

FIG. 16. Comparison between the three methods calculating $\eta^*_{xy,xy}$ in the square geometry: the Einstein-Helfand formula (3) (continuous line), the escape-transport formula (13) (dots), and the chaos-transport formula (25) (crosses) with $\chi=45\sqrt{n}$ for density $n<0.66$, $\chi=100\sqrt{n}$ for $0.67<n<0.75$, and $\chi=150\sqrt{n}$ for $0.76<n$.

V. CONCLUSIONS

In the present paper, we have applied the escape-rate formalism to the computation of shear viscosity in the two-disk model by Bunimovich and Spohn [16].

The escape-rate formalism implies the appearance of a fractal repeller associated with viscosity. We have numerically generated the fractal repeller associated with viscosity in this model and have provided evidence for its fractal character. Using the chaos-transport formula of the escape-rate formalism, we have been able to evaluate the shear viscosity from the positive maximum Lyapunov exponent and the Hausdorff codimension of the fractal repeller of viscosity. The values obtained by using the chaos-transport formula for shear viscosity have been compared with the values obtained by other methods based on the Einstein-Helfand formula, which is equivalent to the Green-Kubo formula as shown in our previous paper [17]. An excellent agreement has been observed between the different methods. This agreement brings an important support to the escape-rate formalism as a method to establish a connection between the transport properties—here of viscosity—and the underlying microscopic chaotic dynamics. The agreement therefore confirms the theoretical results of the escape-rate formalism [7,8].

This confirmation opens perspectives for our understanding of the hydrodynamic modes of shear viscosity. Indeed, in the case of diffusion, the fractal character of the repeller has been shown to imply that the nonequilibrium states are described by singular measures defined in the phase space of the system [10]. These results suggest a similar scenario in the case of viscosity that the nonequilibrium states of a sheared fluid should also be described by singular measures at the phase-space level of description.

The possibility of describing nonequilibrium states by singular measures has been mentioned by Hoover and coworkers in the thermostated-system approach [24] where the nonequilibrium constraints are taken into account by thermostating forces which do not satisfy Liouville's theorem of statistical mechanics. As a consequence, the trajectories of such non-Hamiltonian systems collapse to an attractor by the effect of the average contraction of phase-space volumes and the singular measures supported by the attractor are not compatible with the Hamiltonian character of the microscopic dynamics. Thanks to the escape-rate formalism, these problems are solved and the singular measures we here propose are compatible with Hamiltonian dynamics and its Liouville's theorem.

Our results can be extended to investigate the connection between viscosity and underlying chaos in many-particle systems with a whole spectrum of positive Lyapunov expo-

nents. In many-particle systems, the fractal repeller is characterized by a spectrum of partial fractal dimensions which enter the chaos-transport formula (23). In this way, we can decompose a transport property such as viscosity onto the spectrum of Lyapunov exponents.

The escape-rate formalism also opens perspectives to study viscosity and other transport properties in nanoscopic systems such as nanopipes or atomic and molecular clusters. Indeed, the escape-rate formalism provides a way to define the transport properties already in nanoscopic systems containing a very small number of particles. The escape-rate formalism is particularly appropriate for nanoscopic systems because the transport coefficients can be defined with the escape rate of the Helfand moment out of a finite range of variation. Since the Helfand moment for viscosity can be seen as the center of momenta of the particles, its variations are limited to a finite range in a system containing a finite number of particles. In this way, the transport properties could be studied for nanoscopic systems of increasing size in a similar way as the equilibrium thermodynamic properties have been studied in nanoscopic systems as a function of their size.

We hope to report on these issues in future publications.

ACKNOWLEDGMENTS

The authors thank Professors J. R. Dorfman and G. Nicolis for support and encouragement in this research, and Dr. I. Claus for helpful discussions. S.V. acknowledges the FRIA for financial support. P.G. acknowledges the National Fund for Scientific Research (FNRS Belgium) for financial support.

[1] R. Livi, A. Politi, and S. Ruffo, J. Phys. A **19**, 2033 (1986).
[2] H.A. Posch and W.G. Hoover, Phys. Rev. A **38**, 473 (1988).
[3] H. van Beijeren, J.R. Dorfman, H.A. Posch, and Ch. Dellago, Phys. Rev. E **56**, 5272 (1997).
[4] P. Gaspard and H. van Beijeren, J. Stat. Phys. **109**, 671 (2002).
[5] J.-P. Eckmann and D. Ruelle, Rev. Mod. Phys. **57**, 617 (1985).
[6] E. Ott, *Chaos in Dynamical Systems* (Cambridge University Press, Cambridge, 1993).
[7] P. Gaspard and G. Nicolis, Phys. Rev. Lett. **65**, 1693 (1990).
[8] J.R. Dorfman and P. Gaspard, Phys. Rev. E **51**, 28 (1995).
[9] P. Gaspard and J.R. Dorfman, Phys. Rev. E **52**, 3525 (1995).
[10] P. Gaspard, *Chaos, Scattering and Statistical Mechanics* (Cambridge University Press, Cambridge, 1998).
[11] J.R. Dorfman, *An Introduction to Chaos in Nonequilibrium Statistical Mechanics* (Cambridge University Press, Cambridge, 1999).
[12] H. Kantz and P. Grassberger, Physica D **17**, 75 (1985).
[13] P. Gaspard and F. Baras, Phys. Rev. E **51**, 5332 (1995).
[14] I. Claus and P. Gaspard, Phys. Rev. E **63**, 036227 (2001).
[15] I. Claus, P. Gaspard, and H. van Beijeren, e-print nlin.CD/0309051.
[16] L.A. Bunimovich and H. Spohn, Commun. Math. Phys. **176**, 661 (1996).
[17] S. Viscardy and P. Gaspard, Phys. Rev. E **68**, 041204 (2003).
[18] E. Helfand, Phys. Rev. **119**, 1 (1960).
[19] L.S. Young, Ergod. Theory Dyn. Syst. **2**, 109 (1982).
[20] L.A. Bunimovich and Ya.G. Sinai, Commun. Math. Phys. **78**, 247,479 (1980).
[21] Ya.G. Sinai, Russ. Math. Surveys **25**, 137 (1970).
[22] H. van Beijeren, A. Latz, and J.R. Dorfman, Phys. Rev. E **63**, 016312 (2001).
[23] S.W. McDonald, C. Grebogi, E. Ott, and J.A. Yorke, Physica D **17**, 125 (1985).
[24] W.G. Hoover, C.G. Hoover, W.J. Evans, B. Moran, J.A. Levatin, and E.A. Craig, in *Microscopic Simulations of Complex Flows*, edited by M. Mareschal (Plenum, New York, 1990), p. 199, and references therein.